

Article

Experimental Study of a PowerCore Filter Bed Operating in a Two-Stage System for Cleaning the Inlet Air of Internal Combustion Engines

Tadeusz Dziubak 

Faculty of Mechanical Engineering, Military University of Technology, Gen. Sylwestra Kaliskiego Street 2, 00-908 Warsaw, Poland; tadeusz.dziubak@wat.edu.pl

Abstract: Small dust grains cause a higher intensity of increase in the flow resistance of the fibrous filter bed, which, due to the established value of the permissible resistance, results in a shorter period of operation of the air filter and the vehicle. At the same time, the mass of dust per unit of filtration area takes on smaller values. Such a phenomenon occurs in the two-stage “multicyclone-baffle filter” engine inlet air filtration system. The main objective of this study was to experimentally determine the mass of dust retained per unit of filtration area (dust absorption coefficient k_m) of the PowerCore filter bed operating under two-stage filtration conditions, which cannot be found in the available literature. The original methodology and conditions for determining the dust absorption coefficient k_m of a PowerCore filter bed operating under two-stage filtration conditions are presented. Tests were carried out on the characteristics of filtration efficiency and accuracy, as well as on the flow resistance of a filtration unit consisting of a single cyclone and a PowerCore test filter with an appropriately selected surface area of filter material. During the tests, conditions corresponding to the actual conditions of vehicle use and air filter operation were maintained, including filtration speed and the dust concentration in the air. The experimentally determined dust absorption coefficient of the PowerCore research filters operating in a two-stage filtration system took on values in the range of $k_m = 199\text{--}219\text{ g/m}^2$. The dust absorption coefficient k_m of the PowerCore research filter operating under single-stage filtration conditions reached a value of $k_m = 434\text{ g/m}^2$, which is twice as high. Prediction of the mileage of a car equipped with a single-stage and two-stage “multi-cyclone-partition” filtration system was carried out, showing the usefulness of the experimentally determined dust absorption coefficients k_m .

Keywords: PowerCore filter bed; separation efficiency and accuracy; pressure drop; dust absorption coefficient; two-stage air filter; vehicle internal combustion engine



Citation: Dziubak, T. Experimental Study of a PowerCore Filter Bed Operating in a Two-Stage System for Cleaning the Inlet Air of Internal Combustion Engines. *Energies* **2023**, *16*, 3802. <https://doi.org/10.3390/en16093802>

Academic Editor: Anastassios M. Stamatelos

Received: 3 April 2023
Revised: 24 April 2023
Accepted: 26 April 2023
Published: 28 April 2023



Copyright: © 2023 by the author. Licensee MDPI, Basel, Switzerland. This article is an open access article distributed under the terms and conditions of the Creative Commons Attribution (CC BY) license (<https://creativecommons.org/licenses/by/4.0/>).

1. Introduction

Along with the air drawn in from the atmosphere, engines suck in significant amounts of natural pollutants resulting from environmental activities (e.g., volcanic eruptions, forest fires, peat bogs, dust storms, flower pollen, mold particles, plant spores, bacteria, fungi, mites) and artificial (i.e., anthropogenic) pollutants, the source of which is industry and motorization. Industry is mainly a source of dust and toxic gases, while motorization is a source of toxic gases (e.g., CH, CO, NO_x), lead compounds, PM (particulate matter), dust from the wear of brake friction linings and clutch discs, and dust from the wear of wheel tires and road surfaces. Due to their mass, dirt particles fall to the ground at different speeds, the value of which depends on the particle’s diameter and density. The reciprocal relationship between the drag force of the medium and the gravitational force is also important. The speed of descent increases significantly with increasing grain diameter. Particles smaller than 0.1 μm undergo random Brownian motion, resulting from collisions with gas particles and only slightly from collisions with other dust particles,

whose motion, in turn, is mainly driven by moving gas particles. Particles between 0.1 and 1 μm have settling velocities in still air that are small compared to wind speeds. Particles larger than 1 μm have noticeable but small settling velocities. Particles above about 20 μm have high settling velocities and are removed from the air by gravity and other inertial processes. The approximate settling velocities for particles with a density of 1000 kg/m^3 are 0.1 μm — $4 \times 10^{-7} \text{ m/s}$, 1 μm — $4 \times 10^{-5} \text{ m/s}$, 10 μm — $3 \times 10^{-3} \text{ m/s}$, and 100 μm — $3 \times 10^{-1} \text{ m/s}$ [1]. On the other hand, silica SiO_2 grains (density: 2650 kg/m^3) of 10, 50, and 100 μm fall with velocities of 0.08, 0.19, and 0.7 m/s , respectively. The mixture of many solid contaminants settled on the ground forms road dust, which—as a result of the movement of vehicles or by the wind—is lifted from the ground into the atmosphere, from where it is sucked up by engine intake systems.

The main component of engine inlet air pollution (road dust) is mineral dust, and its main components are silica (SiO_2) and alumina (Al_2O_3). The dust mass share of these two components is in the range of 65–95%, depending on the substrate. The presence of other components in the dust (e.g., Fe_2O_3 , MgO , CaO , K_2O , Na_2O , and SO_3) is at the level of 1–5% [2–4].

Silica and alumina have hardness of 7 and 9 on the Mohs scale, respectively, where diamond—as the hardest mineral—has 10. The mineral grains have a very irregular polyhedral shape with sharp edges. Therefore, they are the main cause of accelerated abrasive wear of two frictionally cooperating engine parts, including the T-P-C (piston–piston rings–cylinder liner) and crankshaft–pan pivot. Excessive wear of the T-P-C association causes an increase in combustion chamber leakage, which is the reason for the “escape” of fresh charge into the crankcase. As a result, there is a decrease in compression pressure and engine power, and an increase in specific fuel consumption and exhaust emissions [5,6].

In order to reduce friction losses and wear on the main components of a piston internal combustion engine, wear-resistant coatings applied to the sliding surfaces of piston rings and cylinder faces are appropriate [7,8]. A significant reduction in friction losses in an internal combustion engine can be achieved by ensuring the continuity of the oil film through appropriate selection of the shape of the sliding surfaces of both the upper and lower sealing rings [9].

Ensuring adequate cleanliness of the inlet air to the internal combustion engines of motor vehicles and work machinery, and thereby minimizing the wear of friction associations and achieving long life of the assemblies, is still an important operational and design problem, especially when tracked vehicles in a column are driven over sandy terrain. Air dust concentrations then take on values of more than 1 g/m^3 . The condition of the ground due to precipitation, the direction of the wind, the conditions in which the vehicles are moving, and the type of running gear cause the dust concentration in the air to reach different values (Table 1).

Table 1. Dust concentrations in the air for different vehicle traffic conditions.

Author	Ambient Conditions	Value (g/m^3)
[10,11]	Moving column of tracked vehicles in dry desert conditions	20
[12]	Dusty environments	0.001–10
[13]	Cars moving on highways	0.0004–0.1
[13]	Moving columns of vehicles on dry, sandy terrain	do 0.03–8
[14]	An all-terrain vehicle moving a distance of several meters behind the column driving on sandy terrain at 30 km/h : A column of tanks;	1.17
	A column of armored personnel carriers;	0.62
	A column of trucks.	0.18

According to the authors of [15], at dust concentrations in the range of $0.05\text{--}0.7\text{ g/m}^3$, visibility is reduced, and when the value of 1.5 g/m^3 is exceeded, visibility becomes zero.

For filtration of the intake air of modern passenger car engines, air filters are used with a filter cartridge, most often made of pleated paper, with a low and limited absorbency (in the range of $150\text{--}250\text{ g/m}^2$), but characterized by high accuracy above $d_p = 2\text{--}5\text{ }\mu\text{m}$ and high separation efficiency above $\varphi = 99.5\%$. A mid-range passenger car requires about $200\text{--}300\text{ m}^3$ of air per hour for the fuel–air mixture. At a dust concentration in the vehicle’s environment of $s = 5\text{ mg/m}^3$, the engine sucks in less than 400 g of dust along with the air over the course of $20,000\text{ km}$, requiring 2 m^2 of filter paper area. Trucks, working and agricultural machinery, and special vehicles are equipped with large-displacement and high-power CI engines, which require an air flow of $2000\text{--}4000\text{ m}^3/\text{h}$ or more. More than 170 kg of dust enters the engine of a special vehicle ($V_{ss} = 38.8\text{ dm}^3$) operated at an average speed of $V = 20\text{ km/h}$ on dirt roads ($s = 1\text{ g/m}^3$) along with the air during a 1000 km run. Stopping such a large mass of dust is possible only through two-stage filters, where the first stage of filtration is an inertia filter (multicyclone, i.e., dozens of cyclones arranged in parallel), and the second is a filter paper cartridge (Figure 1). The essence of the operation of the two-stage filter is that inertia filters are able to separate significant masses of dust from large streams of polluted air (with an efficiency of $86\text{--}97\%$), without an increase in pressure drop, but with a low accuracy below $15\text{--}35\text{ }\mu\text{m}$. This is evident from the literature [16–20], as well as from the single-cyclone tests performed by the author [21,22].

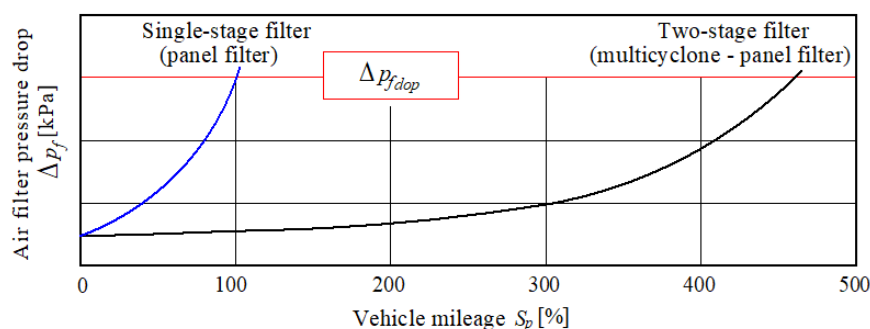


Figure 1. Variation in the pressure drop of a single-stage air filter (paper cartridge) and a two-stage air filter operating in a “multicyclone-paper cartridge” system.

Only a small fraction (about 10%) of the dust mass sucked in with the inlet air reaches the second stage of filtration (paper cartridge). Since the porous baffle has limited absorption capacity, the operating time of the two-stage engine air filtration system to reach the permissible pressure drop of the filter Δp_{fdop} ($5\text{--}8\text{ kPa}$) is much longer than that of the baffle filter alone under the same dusty air conditions, increasing the vehicle’s service interval (Figure 1).

A Multicyclone is a device built of individual cyclones; the diameter of the cylindrical part of the cyclone D does not exceed 40 mm . Several cyclones are set in parallel (side by side) and connected by common plates, which guarantee a common air inlet and outlet. The dust retained in the cyclones is collected in a dust-settling tank, which is a common element for all cyclones.

Multicyclones can be built with return or through-feed cyclones. Due to their simple and robust design, lack of moving parts, and because of their low pressure drops and small changes in pressure during operation, cyclones have become a device that is popularly used for the pre-filtration of air sucked in by vehicles’ internal combustion engines. Cyclones have the advantage of being able to operate under conditions of high dust concentrations in the air and high temperatures. A two-stage (multicyclone–filter cartridge) system for the filtration of air drawn in by an internal combustion engine is shown in Figure 2. The second stage of filtration is a cylindrical filter cartridge with an appropriately sized surface of filter material, arranged in series behind the multicyclone.

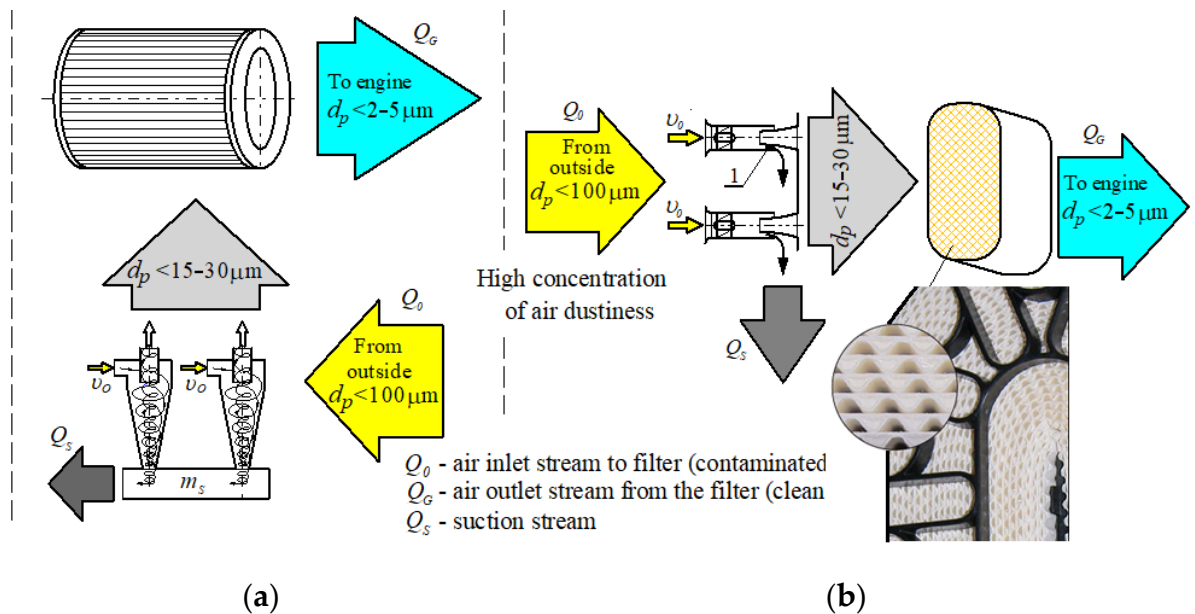


Figure 2. Two-stage (multicyclone–filter cartridge) inlet air filtration system for an off-road vehicle engine: (a) tangential inlet return cyclones–paper cylindrical cartridge, (b) through-feed cyclones with axial inlet–PowerCore cartridge.

The large values of pressure drop (2–2.5 kPa) that tangential inlet return cyclones generate in the engine intake system have recently caused researchers to focus on the development of axial inlet pass cyclones. The overall structure of a through-feed cyclone differs from that of a tangential inlet return cyclone. The basic element of a through-feed cyclone is a cylindrical hull, inside which a swirler is located in its front part, which usually has four blades (vanes) with a helicoidal (helical) surface. When using a multicyclone with through-feed cyclones, it is more advantageous to use a filter cartridge of the PowerCore type (Figure 2b). Air flow then takes place in the same direction, reducing the pressure drop of the entire system.

The PowerCore filter cartridge has a completely different design from previous cylindrical cartridges. It is a monolith constructed of layers of smooth and pleated paper arranged alternately. The resulting parallel channels have either a blinded inlet or a blinded outlet. A channel with a free inlet has a blinded outlet, and vice versa. The resulting design forces air to flow through the channel wall—which is a filter material—into an adjacent channel that has a free outlet. This avoids excessive turbulence and allows the aerosol to flow directly into the filter outlet, reducing the flow resistance.

With the same flow rate, filter cartridges made with PowerCore technology have several advantages; firstly, they are dimensionally 2–3 times smaller than conventional pleated filter paper cartridges made in the form of a cylinder [23,24], and they achieve efficiency $\varphi_f = 99.85\%$ [25–27]. PowerCore cartridges have a higher dust capacity and, thus, a longer life, which means less frequent replacement and lower operating costs.

The air filtration process in the filter cartridge of a single-stage filter proceeds differently from that on the filter cartridge that is the second filtration stage set in series behind the multicyclone. In the case of a single-stage filter, dust directly from the environment flows into the filter cartridge along with the air. These are large dust grains, but not exceeding the value of $d_p = 100 \mu\text{m}$. In a two-stage air filtration system (multicyclone–filter cartridge), the dust at the exit of the cyclone has a different fractional composition than at the inlet to the cyclone. In the multicyclone, dust grains with sizes above $d_p = 15\text{--}35 \mu\text{m}$ are retained, and then small dust grains flow onto the second filtration stage (i.e., paper filter). This is evident from the information presented in the literature [28–31].

Retained in the porous bed (filter paper, non-woven fabric), small dust grains form a more compact—and, thus, less permeable to air—structure. This results in a more rapid increase in flow resistance. As a result, the filter obtains the established value of the permissible resistance Δp_{fdop} much earlier and for a smaller mass of retained dust. At the same time, the mass of dust retained per unit area of filtration takes smaller values. Such a phenomenon was observed during numerical studies of fibrous materials [32–35] and experimental studies of the “cyclone-filter paper” assembly [22,36].

Limitations of the filter’s operation due to the achievement of the permissible value of pressure drop Δp_{fdop} result in a reduction in its service life. This property is important when analyzing the required mileage of the vehicle/air filter operating time.

This property is characterized by the dust absorption coefficient k_m of the filter paper, which can be defined—assuming a uniform distribution of dust over the entire active surface of the test cartridge filter paper—by the following relationship [37–40]:

$$k_m = \frac{m_w}{A_w} \left[\text{g/m}^2 \right], \quad (1)$$

where m_w is the total mass of dust retained by the filter medium around the time of the adopted value of the permissible resistance Δp_{fdop} .

Cellulose-based filter materials loaded with standard dust, the grain size of which usually does not exceed 100 μm , are in the range $k_m = 220\text{--}240 \text{ g/m}^2$ [41–43]. Any other filter material will have a different value of this coefficient. Therefore, for the design of the filter element of a two-stage filter, it is necessary that the operating properties of the filter material are suitable for the operating conditions of the second stage of the air filter, set in series behind the multicyclone.

During the design (i.e., selection of filter paper) of air filters for heavy-duty vehicles’ CI engines, the permissible filtration velocity should not exceed the value $v_{Fdop} = 0.03\text{--}0.06 \text{ m/s}$ [42–44].

For the nominal air demand of the engine Q_{Ns} , and assuming the permissible value of the filtration speed from the above range, the active filter area is then determined from the following relation:

$$A_w = \frac{Q_{Ns}}{3600 \cdot v_{Fdop}} \left[\text{m}^2 \right]. \quad (2)$$

The filter operating time can be determined during in-service testing of complete air filters on a vehicle or during laboratory testing. However, such tests are very expensive, labor-intensive, and complicated. In the available literature, a theoretical relationship is given to determine the operation time τ_p of a two-stage air filter [45]:

$$\tau_p = \frac{A_w \cdot k_m \cdot k_c}{Q_{Ns} \cdot s \cdot (1 - \varphi_m) \cdot \varphi_p} h, \quad (3)$$

where A_w is the active surface area of the filter material of the second stage of filtration (m^2), k_m is the dust absorption coefficient of the filter material at Δp_{fdop} (g/m^2), k_c is the coefficient that takes into account the difference between the parameters of the actual pollutants contained in the engine inlet air and the test pollutants during laboratory testing, Q_{Ns} is the nominal air demand of the engine (m^3/h), s is the average concentration of dust in the air sucked from the environment into the filter (g/m^3), φ_m is the separation efficiency of the first stage of air filtration (multicyclone), and φ_p is the separation efficiency of the filter material of which the filter cartridge is made.

For a constant assumed driving speed V_p (km/h), the distance traveled by the vehicle S_p during τ_p is expressed by the following relation:

$$S_p = \tau_p \cdot V_p \left[\text{km} \right]. \quad (4)$$

Relation (5) then determines the distance traveled by the vehicle until the filter reaches an acceptable resistance Δp_{fdop} :

$$S_p = \frac{A_c \cdot k_m \cdot k_c \cdot V_p}{Q_{Ns} \cdot s \cdot (1 - \varphi_m) \cdot \varphi_p} [\text{km}]. \quad (5)$$

It follows from the presented relationship that its practical use requires knowledge of many data that characterize a particular filter material, including the absorption coefficient k_m , the separation efficiency φ_p , and the coefficient k_c for a specific type of air pollutant. Manufacturers of filter materials only provide data describing their structure with the following parameters: bed thickness, pore dimensions, grammage, mechanical strength, pressure drop (permeability), and density. The efficiency of modern filter materials used in automotive technology is known and takes values in the range of $\varphi_p = 99.5\text{--}99.9\%$. The coefficient $k_c = 1$ when tested with test dust. It follows that the only unknown parameter in Relation (5) is the dust absorption coefficient k_m .

For pleated cellulose-based filter materials operating in a two-stage filtration system, values of the dust absorption coefficient k_m can be found [34,35,46]. Lacking in the available literature are values of the dust absorption coefficient k_m for filter beds of the PowerCore type, which have a different design than pleated beds. Therefore, in the present work, it was decided to partially fill this gap by conducting experimental studies on PowerCore beds operating in two-stage and single-stage systems. To this end, an original and uncomplicated methodology for determining the dust absorption coefficient k_m of filter materials for the second stage of filtration in a two-stage “multicyclone-partition” filter is presented. The methodology involves testing a set in the form of a single cyclone and a test filter medium set in series behind it, which is an appropriately sized section of the actual filter medium. If during the testing of the “filter set” the operating conditions of the test filter cartridge and the cyclone are maintained as they occur during the operation of a complete air filter of real dimensions, the results obtained can be treated as the characteristics of the actual-size filter cartridge.

2. Materials and Methods

2.1. Materials

The subject of experimental and analytical analyses was the filter material from the original PowerCore (Figure 3a) cartridge, from which test filters with a filter area of $A_w = 0.153 \text{ m}^2$ were made and shaped into cylindrical cores (Figure 3b).

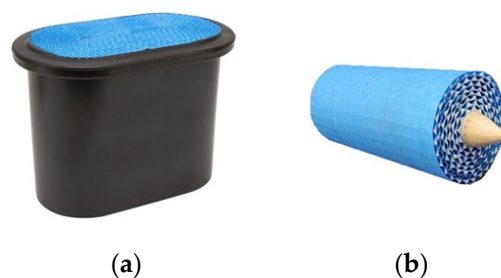


Figure 3. (a) Fabricated research filter; (b) original PowerCore G2 filter cartridge (author’s photos).

The purpose of this study was to determine and compare the filtration properties (separation efficiency and accuracy, pressure drop and dust absorption coefficient k_m) of research filters made from a PowerCore filter bed operating in single-stage and two-stage (in series behind the cyclone) filtration systems.

A pass-through cyclone, which is a component of off-road vehicles’ intake air filters, was used as the first filtration stage of the “cyclone-infiltrator” filtration set (Figure 4).

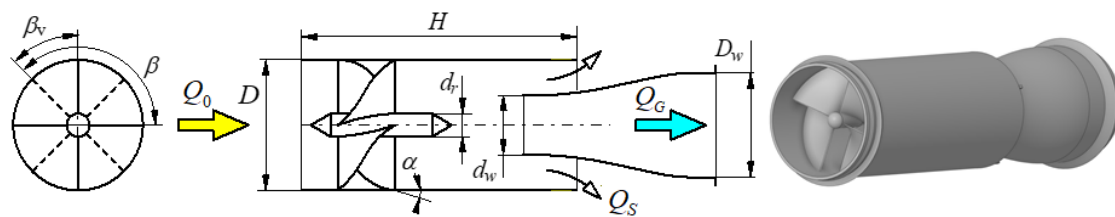


Figure 4. Through-feed cyclone: Q_0 —inlet stream, Q_G —outlet stream, Q_S —dust extraction stream, swirl diameter $D = 36$ mm, height of the cylindrical part of the cyclone $H = 100$ mm, inlet diameter of the outlet tube $d_w = 18$ mm, angle of turn of the guide vanes $\beta = 135^\circ$, angle of overshoot of the guide vanes $\beta_v = 45^\circ$, outlet diameter of the outlet tube $D_w = 36$ mm, diameter of the core $d_r = 6$ mm, outlet angle of the guide vanes $\alpha = 30^\circ$.

The scope of testing of test filters operating with and without a cyclone–filter system included the determination, at a fixed value of the flux Q_{Gmax} , of the following characteristics involving test dust:

- Separation efficiency $\varphi_w = f(k_m)$;
- Filtration accuracy $d_{pmax} = f(k_m)$;
- Pressure drop $\Delta p_w = f(k_m)$.

where k_m is the dust absorption coefficient of the filter material, defined as the total mass of dust m_z retained on 1 m^2 of the active surface of the filter bed until a fixed value of flow resistance is reached.

2.2. Experimental Method

In this study, an experimental research method was applied using a universal stand that was built to determine the performance of single cyclones, research filters, and the characteristics of research filters that are the second stage of filtration (set in series behind a single cyclone)—Figure 5. A single cyclone and a research filter cartridge set directly behind it form a “filter set”.

Immediately upstream and downstream of the test filter was a measuring line, to which a U-tube water-pressure gauge line was connected, which was used to measure the current pressure drop downstream of the test filter and determine the pressure drop Δp_w . The measuring line was terminated with a gauge filter, which was used to collect the mass of m_{AG} dust passed through the test filter. The mass of m_{AG} dust was used to determine the separation efficiency φ_w of the test filter. At the same time, the gauge filter protected the rotameter from dust entering it. The delivery of test dust to the test system was carried out using a vibrating metering device and a stream of compressed air. The dust supplied to the dust chamber was mixed with the inlet air stream Q_0 , and then the contaminated air was sucked into the cyclone or test cartridge.

The dust retained by the cyclone fell by the force of gravity into a sealed settling tank, where it was not stored but was removed on an ongoing basis by means of an additional Q_S flux (suction flux) produced by a special pump. The value of the Q_S flux was determined from the following relation for the assumed value of the suction stage $m_0 = 15\%$:

$$Q_S = Q_G \cdot m_0. \quad (6)$$

The air flow rate Q_G was determined according to Relation (7) for the assumed maximum filtration velocity $v_F = 0.06$ m/s in the filter bed, which for the filters of trucks and special vehicles is recommended in the range $v_F = 0.03$ – 0.06 m/s.

test filters without a cyclone, a dust concentration of $s = 0.5 \text{ g/m}^3$ was used. PTC-D test dust was used, which is a substitute for AC fine test dust in Poland, the chemical and fractional composition of which is shown in Figure 6. The measurement duration, which is the time for uniform dust dosing into the system, was set at $\tau_p = 120 \text{ s}$ during the initial period of filtration (first I) and $\tau_p = 360 \text{ s}$ during the main period (second II) of test filter operation. During the measurement cycle (60 s before the scheduled end of dust dosing), the procedure for measuring the number and size of dust grains in the air behind the research filter was started in the particle counter.

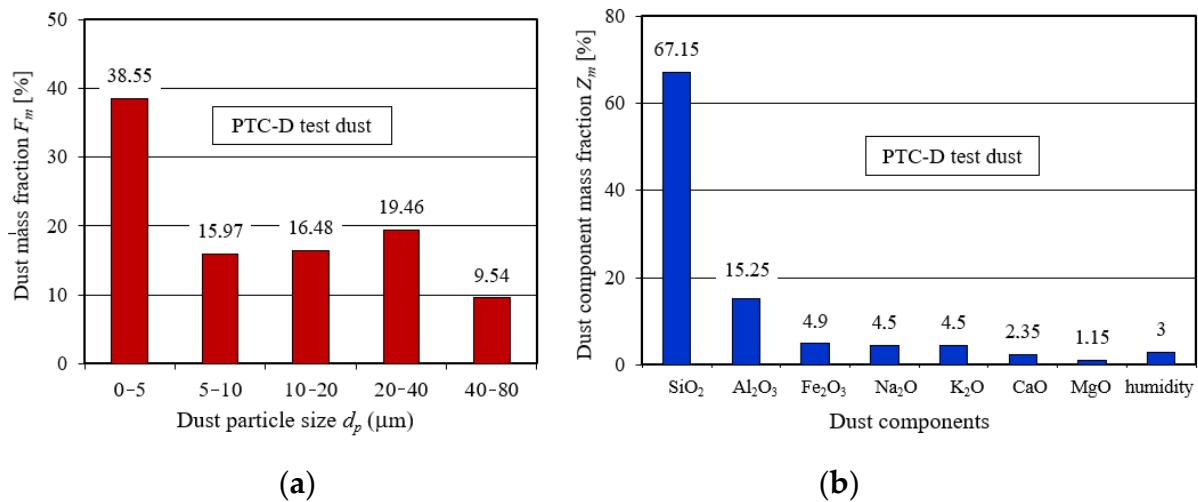


Figure 6. PTC-D test dust: (a) mass proportion of individual fractions in the dust; (b) mass proportions of components in the dust.

After each measurement cycle j , we determined the parameters necessary to determine the efficiency, filtration accuracy, pressure drop, and dust absorption coefficient of the filter cartridge.

1. The pressure drop Δp_{fj} of the filter cartridge was determined as the static pressure drop upstream and downstream of the filter based on the measured (i.e., after the dust dosing was completed) height Δh_{mj} on a U-tube water-pressure gauge.
2. The separation efficiency of the test filter was determined by an indirect method, as the quotient of the mass of dust m_{Fzj} retained by the filter cartridge and the mass of dust m_{Fdj} fed to the filter cartridge during the subsequent measurement cycle, based on the following relation:

$$\varphi_j = \frac{m_{Fzj}}{m_{Dj}} = \frac{m_{Fzj}}{m_{Fzj} + m_{Aj}} 100\%. \quad (8)$$

3. The dust absorption coefficient k_{mj} of the tested filter material was determined from the following relationship:

$$k_{mj} = \frac{\sum_{j=1}^n m_{Fzj}}{A_w} \left[\text{g/m}^2 \right]. \quad (9)$$

4. The N_{pi} number of dust grains passing through the test filter (located in the air stream downstream of the filter) was determined in measurement intervals bounded by fixed diameters ($d_{pimin} - d_{pimax}$).
5. The filtration accuracy was determined as the largest dust grain size $d_{pj} = d_{pmax}$ in the air stream downstream of the filter.
6. The percentage of each dust grain fraction in the air stream downstream of the filter for a given measurement cycle was calculated from the following relation:

$$U_{pi} = \frac{N_{pi}}{N_p} = \frac{N_{pi}}{\sum_{i=1}^{32} N_{pi}} 100\%, \quad (10)$$

where $N_p = \sum_{i=1}^{32} N_{pi}$, which is the total number of dust grains that passed through the test filter (from all measurement intervals) during the measurement cycle.

According to the above methodology, we determined the filtration characteristics (separation efficiency $\varphi_w = f(k_m)$ and filtration accuracy $d_{pmax} = f(k_m)$, as well as pressure drop $\Delta p_w = f(k_m)$) of research filters made from a PowerCore bed working in one-stage and two-stage systems. The tests were carried out until the filter medium reached the assumed value of acceptable resistance $\Delta p_{fstop} = 3$ kPa.

2.3. Analytical Method

An analytical method was used to explain the phenomenon of changes in the flow resistance of the filter bed depending on grain size, which involved analyzing the arrangement of dust grains in a compact structure. Mineral dust drawn in with air has an irregular grain shape and is characterized by high polydispersity in the range up to 100 μm . Therefore, a proxy diameter is adopted for theoretical considerations. Most often, the diameter of dust grains is assumed to be spherical. Figure 7 shows a slice of the deposit model in the form of a cube with side d formed by regularly arranged spheres of equal diameter d .

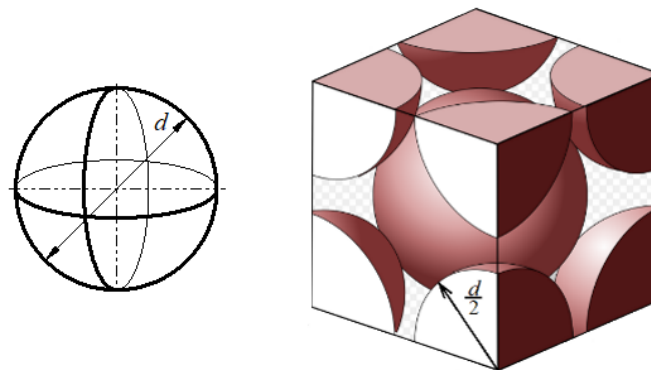


Figure 7. Bed model of similar spherical particles.

The volume V_1 of the space between the particles is equal to the volume V of the cube with side d minus the volume V_2 occupied by the particles, according to the following equation:

$$V_1 = V - V_2 \quad (11)$$

$$V_1 = d^3 - \left(\frac{4}{3} \pi \left(\frac{d}{2} \right)^3 \right) \quad (12)$$

$$V_1 = d^3 \left(1 - \frac{\pi}{6} \right). \quad (13)$$

From the above equation, it follows that the volume V_1 of the space between the particles depends only on the diameter d of the particles in the third power. The volumes V_1 between successive particles form spaces that, when connected together, form a channel d_e for air flow.

At the same time, as the diameter d of the particles decreases, the number of microchannels d_e distributed over the filter area also increases, in proportion to $1/d^2$, since the total dimensions of the filter area do not change. Thus, the total cross-section through which the air flows also does not change, from which it follows that the average air velocity in the microchannels does not change and is independent of d .

The pressure drop Δp of a filter bed laden with dust particles can be described by a modified Darcy–Weisbach formula:

$$\Delta p = \lambda(Re) \frac{g_w}{d_\varepsilon} \frac{\rho}{2} v_\varepsilon^2, \quad (14)$$

where ρ is the density of the fluid, λ is the coefficient of friction, g_w is the thickness of the filter bed, d_ε is the hydraulic diameter of the channels formed by the particles, and v_ε is the actual velocity in the channels between the particles.

It follows from the above relationship that the flow resistance of the filter bed is directly proportional to its thickness g_w , fluid density ρ , and actual velocity v_ε in the channels between the particles, and inversely proportional to the conventional diameter d_ε of the channels formed by the particles. Assuming an invariant value of the thickness of the filter bed g_w and the velocity in the channels between the particles v_ε , the flow resistance then depends on the conventional diameter d_ε of the channels formed by the particles.

3. Results and Discussion

The characteristics of separation efficiency $\varphi_w = f(k_m)$, pressure drop $\Delta p_w = f(k_m)$, and filtration accuracy $d_{pmax} = f(k_m)$ as a function of the dust absorption coefficient k_m of two specimens of PowerCore bed test filters (No. 1 and No. 2), which operated in the “filter set” as the second filtration stage (after the through-feed cyclone), are shown in Figure 7. The obtained characteristics had a similar course and values. Due to the achieved values of separation efficiency, the operating time of the studied filters can be conventionally divided into two periods: The first period (i.e., initial filtration) is characterized by small values of separation efficiency, which systematically increase (sometimes very sharply) with the amount of dust mass retained by the filter bed and, thus, the increase in the dust absorption coefficient k_m . The initial filtration period lasts from the start of the filtration process until the filter material reaches the maximum set value of separation efficiency. In the case of the conducted research, the zone of separation of the two periods was assumed at the moment when the filters reached the separation efficiency $\varphi = 99.5\%$. This value was achieved by the filters at similar values of the dust absorption coefficient i.e., filter No. 1: $k_{m1} = 8.87 \text{ g/m}^2$; filter No. 2: $k_{m2} = 12 \text{ g/m}^2$. After the first measurement cycle, the separation efficiency of both filters reached similar values: research filter No. 1 reached $\varphi_{wc1} = 96.6\%$, and filter No. 2 reached $\varphi_{wc2} = 95.8\%$ (Figure 8), showing the homogeneity of the filter bed and the high accuracy of the research filters. During the tests, the cyclone efficiency was at 85.2%. During the tests, the cyclone’s efficiency was 85.2%, and its pressure drop did not exceed $\Delta p_c = 0.6 \text{ kPa}$.

Following the initial filtration period (I), the second period of operation of the PowerCore filter—called the main period (II)—was characterized by a course of efficiency ($\varphi_w = 99.7\text{--}99.99\%$) and filtration accuracy ($d_{pmax} = 3\text{--}6 \text{ }\mu\text{m}$) stabilized at a certain level, and a slow increase in the pressure drop. When the assumed flow resistance $\Delta p_w = 3 \text{ kPa}$ was reached, the filters obtained the dust absorption coefficient k_m at similar levels, i.e., filter No. 1: $k_m = 219 \text{ g/m}^2$, and filter No. 2: $k_m = 199 \text{ g/m}^2$. The data from the literature show that standard pleated cellulose-based filter materials operating in a two-stage system achieve an absorption coefficient of $k_m = 90 \text{ g/m}^2$, which is half that of PowerCore filter beds operating under the same conditions, which may be due to the possibility of accumulation of additional dust mass inside the channels of the PowerCore bed, as shown in Figure 9. Once the filter bed (walls of the channel) has been saturated with dust, as the operation of the filter continues, the dust accumulates inside the channel, which acts as a kind of reservoir. Figure 9b shows the dust accumulated inside the channels of the PowerCore filter under test. Thus, the absorption capacity of the filter bed is enlarged. The dust settles at the bottom of the channel, and its level rises. Thus, the free filter area decreases, causing an increase in the flow velocity through the channel walls, which results in an increase in the filter’s flow resistance (Figure 8).

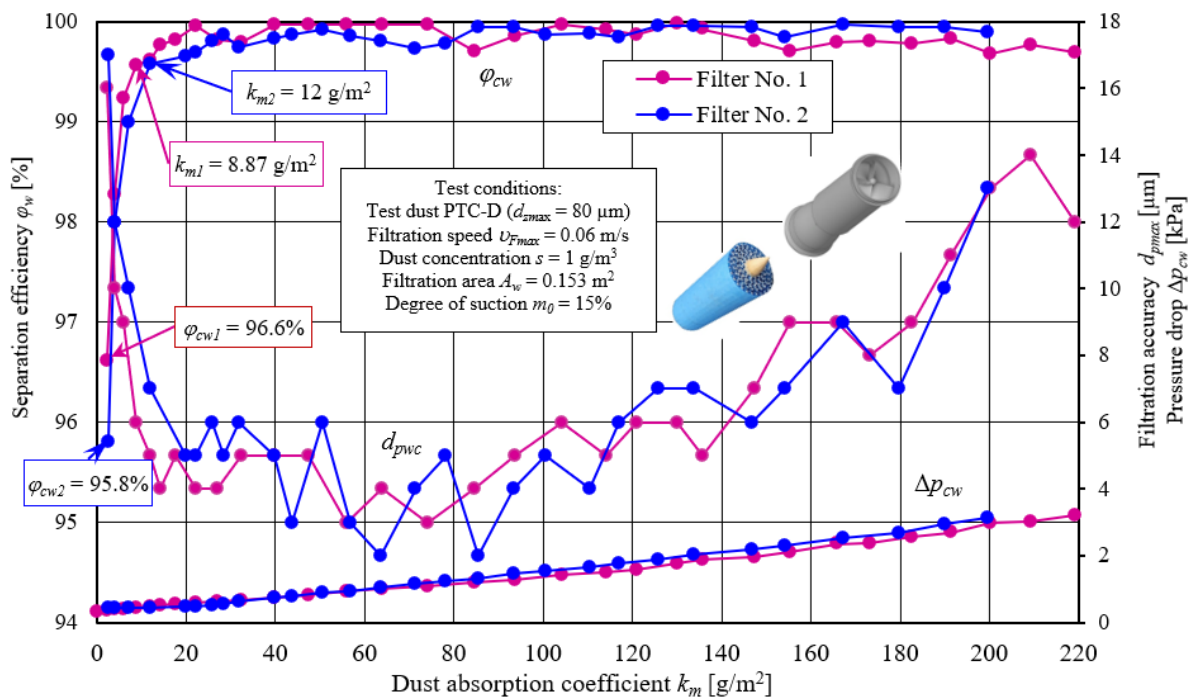


Figure 8. Characteristics: separation efficiency $\varphi_w = f(k_m)$, pressure drop $\Delta p_w = f(k_m)$, and filtration accuracy $d_{pmax} = f(k_m)$ as a function of the dust absorption coefficient k_m of filter beds working in the “filter set” as the second filtration stage (after the through-feed cyclone).

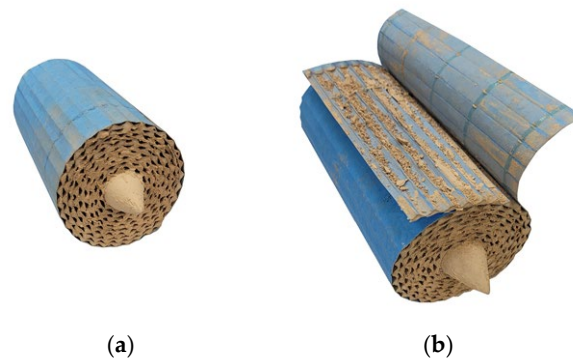


Figure 9. PowerCore filter after testing with test dust: (a) view of the filter from the side of the air and dust inlet; (b) dust accumulated in the bed channels.

Associated with changes in efficiency were the maximum sizes of the dust grains d_{pmax} in the air behind the filter under test. There was a sharp decline, from $d_{pmax} = 17 \mu\text{m}$ after the first measurement to $d_{pmax} = 4\text{--}5 \mu\text{m}$ when the filter reached an efficiency of 99.5%, establishing the end of the first stage of filtration. In the second stage of the filter’s operation, the separation efficiency was maintained at 99.5–99.9%, and the maximum grain size took on values in the range of $d_{pmax} = 3\text{--}6 \mu\text{m}$. After the filters achieved a dust absorption coefficient of $k_m = 150 \text{ g/m}^2$ and a pressure drop of $\Delta p_{wc} = 2.5 \text{ kPa}$, increasingly larger dust grains d_{pmax} and a slight decrease in separation efficiency were registered in the exhaust air. As soon as the filters achieved a pressure drop of $\Delta p_{cw} = 3 \text{ kPa}$, dust grains of $d_{pmax} = 14 \mu\text{m}$ were found in the exhaust air.

For the process of aerosol filtration in fiber baffles, the phenomenon of continuous influx and retention of dust grains on the surface of individual fibers is characteristic. This is mainly the effect of inertial, direct trapping, and diffusion mechanisms. Settling dust grains form characteristic dendrites, which grow to a considerable size, filling the free spaces (i.e., pores) between fibers. Thus, the free field of air flow decreases, which causes

an increase in velocity between fibers. As a result, there is an increase in the pressure drop, which is a function of velocity in the second power. The increase in the mass of dust accumulated in the filter bed causes the pressure drop to increase (Figure 8). Due to the small thickness of the filter papers ($g_p = 0.4\text{--}0.8\text{ mm}$), they have a limited dust absorption capacity. When this is exhausted, the dust settles on the surface of the bed in the form of a “filter cake”, which manifests itself in an additional increase in flow resistance. The large pressure drop downstream of the filter and the high velocity of air flow in the narrow channels between the fibers can cause dust grains to be locally detached from the formed dendrites and transported toward the outlet. These can be dust grains of considerable size. In the case of the studied filters, the beginning of this process was noticed when the value of the pressure drop behind the filter reached about $\Delta p_f = 2.5\text{ kPa}$.

Figure 10 shows a comparative analysis of test filter No. 1 operating in a two-stage system (after the cyclone), and of test filter No. 3 with the same parameters but operating in a single-stage system. The characteristics of the efficiency and accuracy of filtration of both filters in the initial period were similar with respect to the course and values. It can be seen that there was a more intense increase in the pressure drop of the filter operating in a two-stage system (downstream of the cyclone). The value $\Delta p_f = 3\text{ kPa}$ was reached by this filter after loading the bed with dust $k_m = 219.2\text{ g/m}^2$. For the research filter operating in a single-stage system, the value of $\Delta p_f = 3\text{ kPa}$ was reached after obtaining a dust load of $k_m = 434.2\text{ g/m}^2$, which is twice as much. This is because smaller dust particles more quickly form dendrites on the fibers, which fill the free spaces (i.e., pores) in the fiber bed, and the flow of air through the layer of dense dust grains is hindered. Hence, the greater pressure drop, which grows more intensively and limits the filter’s operating time and the car’s mileage.

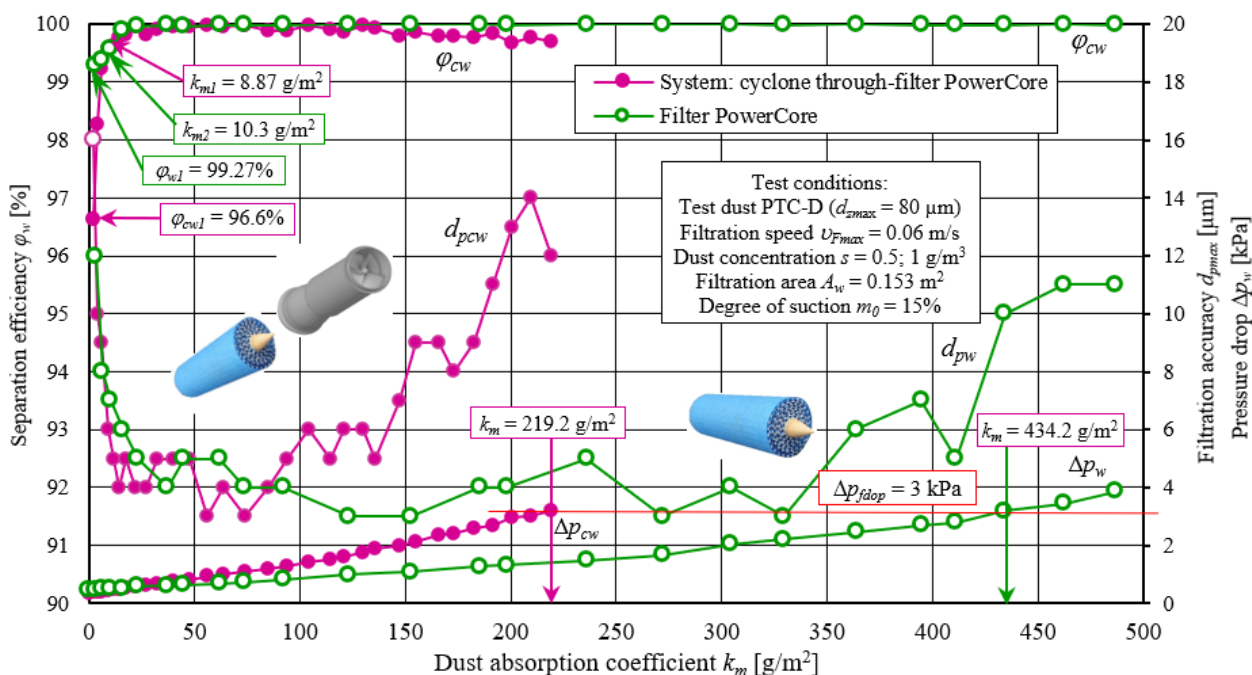


Figure 10. Characteristics of efficiency $\varphi_w = f(k_m)$ and accuracy $d_{pmax} = f(k_m)$ of filtration and flow resistance $\Delta p_w = f(k_m)$, depending on the k_m factor of the PowerCore filter bed tested in the “cyclone-test cartridge” filter set, and without cyclone.

Figure 11 shows the predicted mileage (for different values of dust concentration in the air) of a diesel truck equipped with filters with a single-stage filtration system (PowerCore filter) and with a two-stage system (cyclone–PowerCore filter). Calculations were carried out using Relation (2), along with the dust absorption coefficient k_m of the PowerCore filter and the separation efficiency values of the cyclones φ_m and the PowerCore filter φ_w ,

determined experimentally during the tests. Regardless of the air filtration system present in the vehicle, as the dust concentration in the air increased, the mileage of the vehicle to reach the permissible resistance decreased, with higher mileage values obtained by the vehicle with a two-stage filtration system.

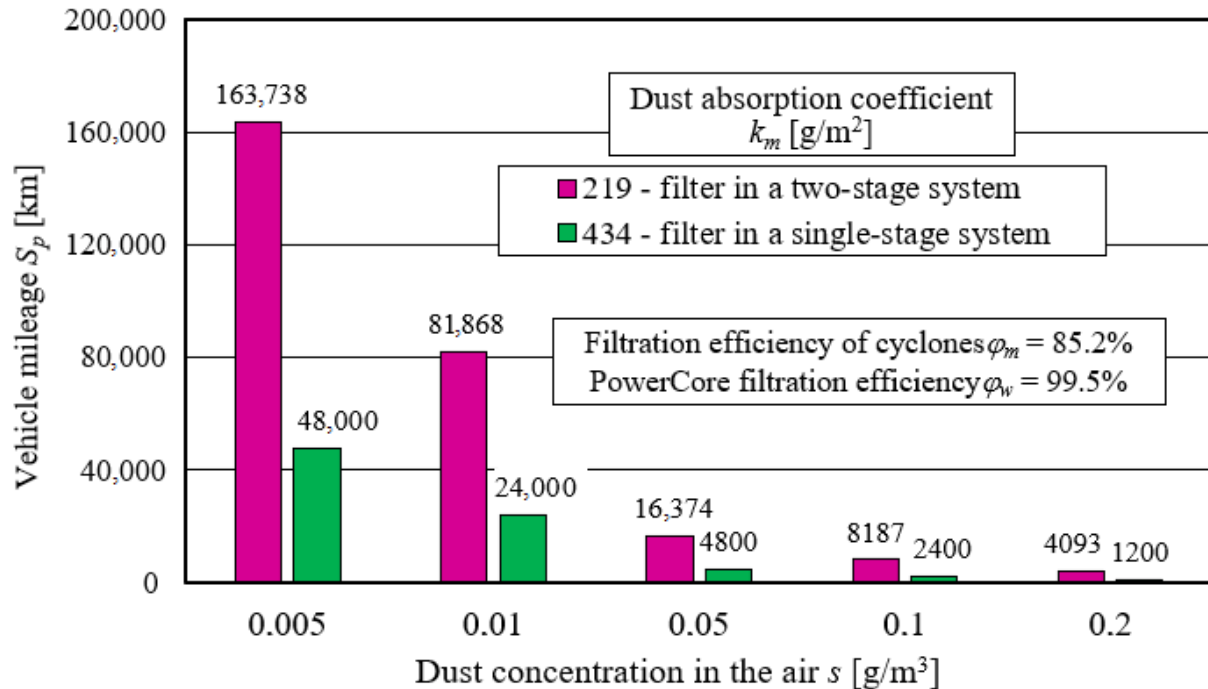


Figure 11. Projected mileage of the car to reach $\Delta p_{fdop} = 3$ kPa under different operating conditions (dust concentration in the air) with an air filter operating in single-stage and two-stage filtration systems.

A vehicle equipped with a PowerCore single-stage filtration system, for a dust concentration of $s = 5 \text{ mg}/\text{m}^3$ and a dust absorption coefficient of $k_m = 434 \text{ g}/\text{m}^2$, achieves a projected mileage of about 48,000 km. The same vehicle, equipped with a two-stage “PowerCore multicyclone-filter” filtration system, for a dust concentration of $s = 5 \text{ mg}/\text{m}^3$ and a much lower ratio of $k_m = 219 \text{ g}/\text{m}^2$, achieves three times the mileage (more than 160,000 km) when the filter reaches the permissible resistance value $\Delta p_{fdop} = 3$ kPa.

To analyze the mileage of vehicles with two-stage and single-stage systems, the pressure drop (3 kPa) on the filter cartridge was assumed to be the same. In the two-stage system, there is an additional pressure drop across the cyclones. In the case of the tested two-stage system, the pressure drop on the through-feed cyclone reached $\Delta p_c = 0.6$ kPa at a nominal air flow rate of $Q_{wmax} = 34 \text{ m}^3/\text{h}$. In order to maintain the same operating conditions of filter materials in both systems (single-stage and two-stage), the operation of the filter operating in the two-stage system should be limited by the permissible resistance of $\Delta p_{fdop} = 3.6$ kPa. Obviously, a higher pressure drop on the filter means additional energy losses from the engine. From the available literature, it is known that the values of the permissible resistance of air filters of trucks and special vehicles are in the range $\Delta p_{fdop} = 6\text{--}8$ kPa.

Projecting the mileage of a vehicle equipped with a filter with a two-stage filtration system (cyclones–baffle), and using a dust absorption coefficient with the same value as for a single-stage filter ($k_m = 434 \text{ g}/\text{m}^2$), results in an artificial extension of this mileage. For a dust concentration of $s = 0.005 \text{ g}/\text{m}^3$, the vehicle mileage is extended to 324,328 km, i.e., by 100%. Such calculations are inappropriate and misleading. Therefore, it is expedient to conduct research to determine the actual dust absorption coefficient k_m of the filter material proposed for operation in a two-stage system, which can then be used to determine the real mileage of the vehicle.

The number of dust grains found in the cyclone’s inlet air stream, and before and after the test filter operating in the “cyclone-inlet” set, in successive measurement cycles for different values of the dust absorption coefficient k_m is shown in Figure 12. It was found that with the increase in separation efficiency in each successive measurement cycle, there was a decrease in the total number N_p of dust grains in the air after the test filter. A clear relationship can be seen between the size of the grains d_p and their number N_p . As the size of the dust grains increases, their number decreases until they disappear completely. Located in the last size interval, grains (or a single grain) have the largest size $d_p = d_{pmax}$ (Figure 12). It was assumed that the dust grain with the largest size d_{pmax} located in the exhaust air stream from the test filter expresses the filtration accuracy of the filter material in measurement cycle j . In the exhaust air stream from the cyclone, there were dust grains whose number had decreased significantly compared to the number of grains in the air before the cyclone. This applies to dust grains above 3 μm . The larger the dust grains, the more effectively they are retained by the cyclone. If we denote cyclone efficiency as the quotient of the number of dust grains retained ($N_{pu} - N_{pw}$) and delivered to the N_{pu} system, dust grains of 5 μm were retained by the cyclone with 53.6% efficiency, 10 μm grains achieved 86.8% efficiency, and 20 μm grains had 97.2% efficiency. The cyclone’s increasing separation efficiency was due to the increasing inertial force of grains with increasing volume and, thus, mass. Grains larger than 35 μm were retained by the cyclone with 100% efficiency. Proceeding in a similar manner, it was determined that after the first measurement cycle, dust grains with a size of 10 μm were retained by the test filter material with 99.5% efficiency.

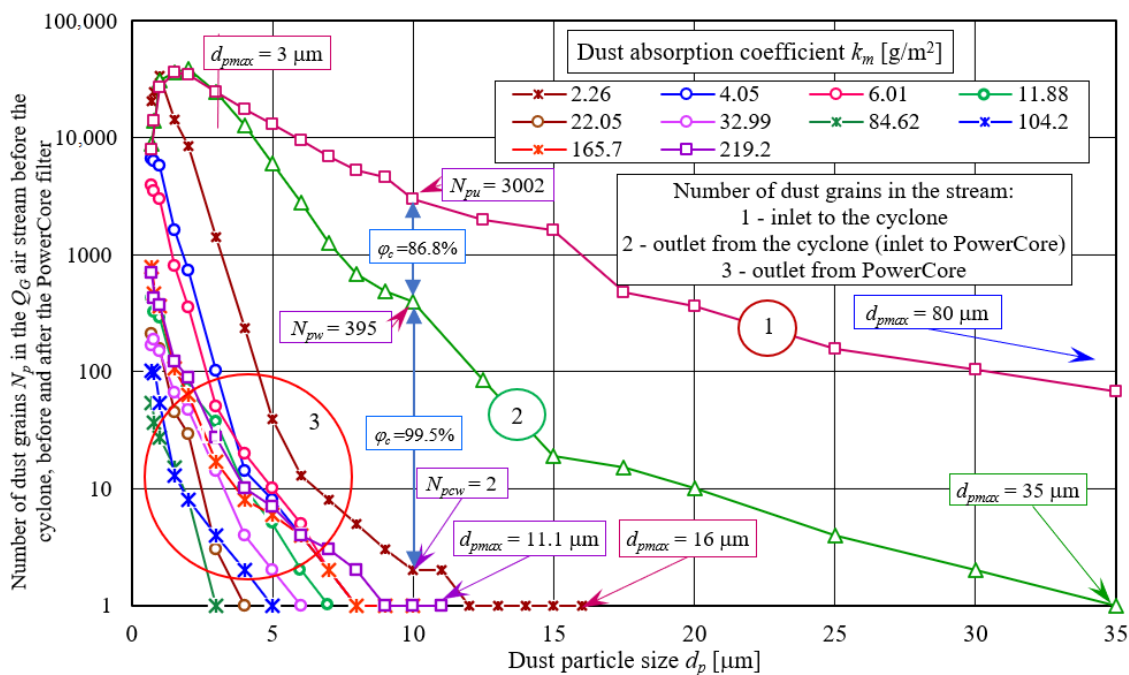


Figure 12. The number of dust grains present in the cyclone’s inlet air stream, upstream and downstream of the PowerCore test filter operating in the “cyclone-test filter” set, in successive measurement cycles for different values of the dust absorption coefficient k_m .

The granulometric composition of dust in the air stream shows the change in the numerical shares of U_p determined by Relation (5) as the size of the dust grains d_p increased. The granulometric composition of dust in the air stream flowing into and out of the cyclone was similar in terms of the course, but there were significant differences as to the values (Figure 13). As the size of the dust grains d_p increased, there was a rather sharp increase in their U_p numerical shares, reaching a maximum at $d_p = 1.5 \mu\text{m}$, followed by a gentle decrease. The U_{pc} number shares of dust grains in the air behind the cyclone were found to

be larger in the range of 0.7–3.8 μm and smaller above 3.8 μm than the U_{pc} number shares of dust in the air entering the cyclone. As a result of the filtration process in the cyclone, larger grains (above 3.8 μm) were separated, resulting in a decrease in their shares of the total number of dust grains and an increase in the shares of dust grains with sizes below 3.8 μm , with this value being a conventional limit for the purposes of this research. For example, the share of dust grains with a size of 2 μm in the air behind the cyclone increased from $U_{p0} = 16.5\%$ to $U_{pc} = 20.7\%$, while the share of dust grains with a size of 6 μm in the air behind the cyclone decreased from $U_{pc} = 4.56\%$ to $U_{p0} = 1.59\%$. Another filtration stage (PowerCore filter) significantly changed the granulometric composition of the dust. In the air downstream of the filter there were mainly smaller dust grains—less than 3.8 μm ; hence, their shares were high. The proportion of dust grains with a size of 1 μm was $U_{p1} = 32.6\%$ after the first test cycle and $U_{p5} = 37.4\%$ after cycle No. 5.

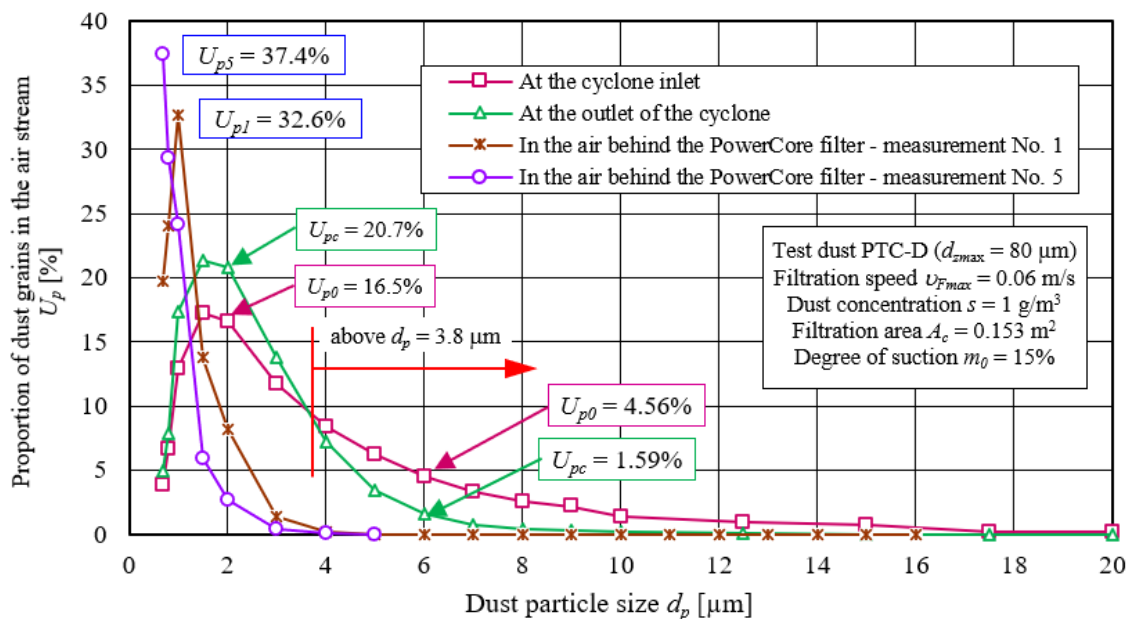


Figure 13. Granulometric composition of dust in the air stream before and after the cyclone and the PowerCore filter.

The low efficiency and accuracy of air filtration by fiber filters is characteristic of their initial stage of operation. This phenomenon occurs in the engine intake system after replacing a contaminated filter element with a new one. This is an unfavorable phenomenon, as the engine's inlet air stream may then contain dust grains of considerable size, which can cause accelerated wear of the internal combustion engine's components. According to the authors of [9–11,47], dust grains with diameters of more than 1 μm are the cause of surface wear, and dust grains with diameters of more than 5 μm are the cause of accelerated wear of two frictionally cooperating engine components. Consequently, such filtration accuracy is required of intake air filters for internal combustion engines. From the above, it follows that the engine's air filter cartridge should not be replaced too often, except for when there is a loss of its filtering properties. The criterion for replacing the air filter cartridge is the achievement of the manufacturer's set value of acceptable resistance. Therefore, the test results obtained by the author are essential for making the right decision as to when to service the air filter. At the final stage of operation of the tested filters (above $\Delta p_f = 2.5$ kPa), dust grains were noted, the size of which ($d_{pcw} = 14$ μm) could cause accelerated wear. From the above analysis, it follows that the air filters should not be used above the specified pressure drop value. Based on the test results obtained, it is reasonable to believe that in the case of the PowerCore filters tested, this value is above $\Delta p_f = 2.5$ kPa.

Although the dust absorption capacity of the filter material operating in a two-stage “cyclone-filter test” filtration system is lower than that of the same material operating in a single-stage system, the operating time of the two-stage system until the permissible resistance $\Delta p_f = 3$ kPa is reached is longer. This was confirmed by the results of the characteristics separation efficiency $\varphi_w = f(m_D)$, pressure drop $\Delta p_w = f(m_D)$, and filtration accuracy $d_{pmax} = f(m_D)$ as a function of the mass of dust m_D delivered to the “cyclone-test filter” filtration system and directly to the PowerCore test filter (Figure 14).

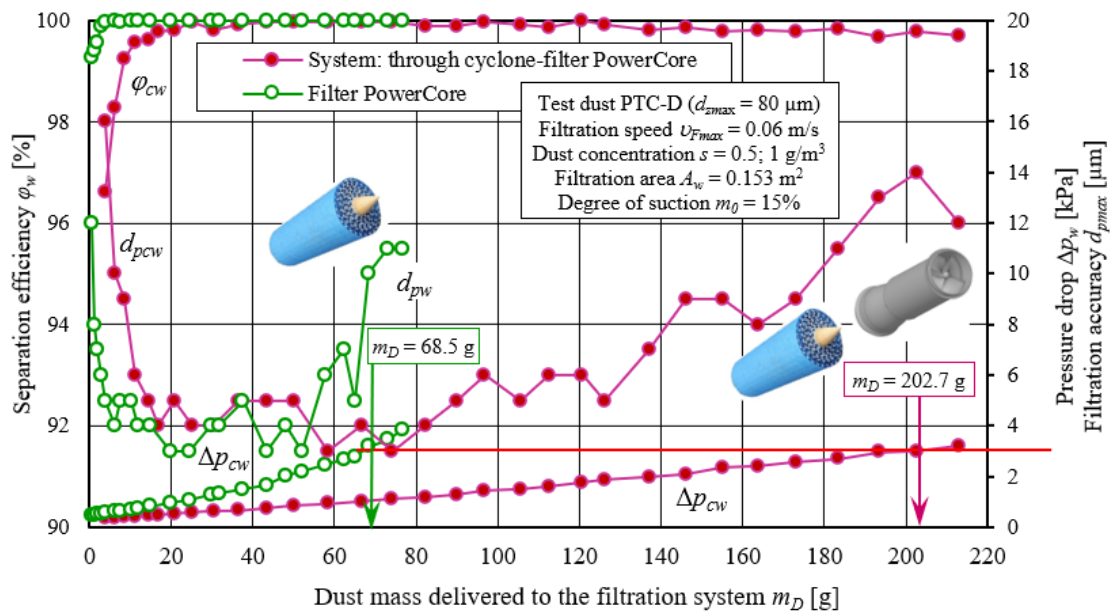


Figure 14. Characteristics: separation efficiency $\varphi_w = f(m_D)$, pressure drop $\Delta p_w = f(m_D)$, and filtration accuracy $d_{pmax} = f(m_D)$ as a function of the mass of dust m_D delivered to the two-stage system “cyclone-filter research PowerCore” and the single-stage system (directly to the research filter PowerCore).

From the presented characteristics, it can be seen that the achievement of the permissible resistance of 3 kPa by the test filter operating in the “cyclone-test filter” system occurs after 202.7 g of dust is supplied to the system. If the test filter operates individually, it achieves a pressure drop of 3 kPa after delivering only 68.5 g of dust. This has a definite impact on the vehicle’s mileage, especially when it is operated under conditions of high dust concentration in the air. The filter’s achievement of the permissible resistance is a prerequisite for its service, i.e., filter element replacement. Although the filter material working in series behind the multicyclone has a lower absorbency, the operating time of the “multicyclone-pore-partition” filter system to reach the permissible resistance is much longer than that of the same cartridge working individually, which is the primary advantage of two-stage filtration. This explains the need for two-stage filters in vehicles operated under conditions of high dust concentration in the air.

If the first stage of filtration of the inlet air to the engine is an inert filter (multicyclone) and the second is a filter cartridge made of fibrous material, then most (i.e., more than 90%) of the dust supplied to the system is retained by the multicyclone. In the case of the tested “cyclone-filter PowerCore” set, the cyclone efficiency was at the level of about 84.6%. Thus, only 15% of the dust mass that was introduced into the “multicyclone-filter” filtration system reached the filter cartridge. The retained dust accumulates in the settling tank or is removed from it on an ongoing basis. During the tests, ejective (ongoing) removal of dust from the cyclone settling tank was used, with a suction rate of $m_0 = 15\%$. Therefore, with a constant flow of air to the engine, the flow resistance of the multicyclone is unchanged—in contrast to baffle filters, where the retained mass causes an increase in flow resistance at the same time.

The increase in flow resistance of a cartridge operating in a two-stage system (cyclone-test filter) is more intense, despite the same mass of dust being retained by the bed per unit area (Figure 10). In the case of two-stage filtration, small dust particles accumulate on the filter bed, which form dendrites on the fibers that grow faster than when the bed is loaded with larger particles. Small dust grains, which make up a much larger percentage of the total number of particles entering the filter when the bed is operated with an upstream cyclone, penetrate the filter paper structure much more easily and fill it more tightly compared to larger-diameter grains. Free spaces are created between the charged dust particles, through which air flows. However, the spaces between small grains are much smaller than those between large dust grains, increasing the velocity of aerosol flow through them and, thus, increasing the flow resistance.

The volume V_1 of space between particles of equivalent diameter $d = 80 \mu\text{m}$, according to Relation (13), takes the following value:

$$V_1 = d^3 \left(1 \frac{\pi}{6}\right)$$

$$V_{1(80)} = 80^3 \left(1 \frac{\pi}{6}\right)$$

$$V_{1(80)} = 267,946.7 \mu\text{m}^3.$$

For smaller and smaller particle diameters d , the volume V_1 of space between particles takes on smaller and smaller values. The volume V_1 of space between particles with an equivalent diameter of $d = 20 \mu\text{m}$, which is four times smaller, has a value of $V_{1(20)} = 4186.7 \mu\text{m}^3$, which is 64 times smaller than for $d = 80 \mu\text{m}$. For $d = 8 \mu\text{m}$, $V_{1(8)}$ is 1000 times smaller, and for $d = 2 \mu\text{m}$, $V_{1(2)}$ is 64,000 times smaller.

From the Darcy–Weisbach relation (Relation (14)) describing the pressure drop Δp of a filter bed loaded with dust particles, it follows that the flow resistance is directly proportional to g_w , ρ , and velocity v_ϵ , and inversely proportional to the conventional diameter d of the channels formed by the particles. For a filter bed loaded with dust particles of small diameters, the conventional diameter d_ϵ of the channels formed by the particles will take smaller values, resulting in an increase in flow resistance. This is the main reason for the increase in pressure drop with decreasing particle size.

In addition, particles with smaller and smaller diameters have a higher and higher ratio of surface area A_c to volume V_c . Consequently, they have a higher resistance and pressure drop per unit volume (i.e., mass of particles). The ratio of the surface area A_c of a particle with the shape of a sphere to its volume V_c is expressed by the following relation:

$$a_g = \frac{A_c}{V_c} = \frac{6}{d_p}. \quad (15)$$

If we take particles with different equivalent diameters for analysis (i.e., $d_p = 80, 50, 20, 10, 2.0, 1.0,$ and $0.7 \mu\text{m}$), the ratio of particle area to volume is then $a_g = 0.075, 0.12, 0.3, 0.6, 3, 6,$ and 8.57 , respectively.

4. Conclusions

In this paper, an experimental study of PowerCore deposits operating in two-stage and single-stage systems was carried out to determine the characteristics of separation efficiency, accuracy, and pressure drop depending on the dust absorption coefficient. To this end, an original and uncomplicated methodology for determining the dust absorption coefficient of k_m filter materials for the second stage of filtration in a two-stage “multicyclone-partition” filter is presented. The methodology consists of testing a set in the form of a single-pass cyclone and a PowerCore test filter medium set in series behind it, which is an appropriately sized section of the actual filter medium. The following conclusions were obtained from the testing and analysis:

1. PowerCore filter beds operating in a “cyclone-pore barrier” system achieve an absorption coefficient of $k_m = 219.2 \text{ g/m}^2$, which is twice as low as when operating in a single-stage filtration system—undoubtedly influenced by the small dust grains resulting from the cyclone filtration process.
2. PowerCore filter beds operating in a two-stage system achieve more than twice the absorption coefficient of standard pleated cellulose-based filter materials, whose $k_m = 90 \text{ g/m}^2$, which may be due to the possibility of dust accumulating inside the channels of the PowerCore bed.
3. Filter materials operating in the “multicyclone-porous baffle” system are characterized by a more intensive increase in flow resistance, which has a direct impact on reducing the operating time of the air filter to reach the permissible resistance, thereby reducing the mileage of the vehicle. This is the result of the formation of a more compact and tight structure from small-diameter dust grains, which have a higher ratio of surface area A_c to volume V_c than larger-diameter grains and, therefore, have a higher resistance and pressure drop per unit volume (mass of dust particles).
4. Forecasting the mileage of a vehicle equipped with a filter with a two-stage filtration system (cyclones-baffle), and using a dust absorption coefficient with the same value as for a single-stage filter ($k_m = 434 \text{ g/m}^2$), results in an artificial extension of mileage by more than 100%, which is inappropriate and misleading. Therefore, it is expedient to conduct research to determine the actual dust absorption coefficient k_m of the filter material proposed for two-stage operation, which can then be used to determine the real mileage of the vehicle.
5. The low ($\varphi = 95.8\text{--}96.6\%$) efficiency of the filter material and the presence of large ($d_{pmax} = 12\text{--}16 \text{ }\mu\text{m}$) dust grains in the purified air during the initial but short period of operation of the baffle filter may affect the accelerated wear of the engine associations working together in a tray—especially the piston–piston ring–cylinder (P-PR-C) association. Dust grains of similar size can also be located behind the air filter when it exceeds a certain pressure drop value. In the case of the tested bed, this value is about 2.5 kPa. Therefore, the use of the air filter after exceeding the specified value of the permissible resistance is not advisable.
6. Although the filter material working in series behind the multicyclone has a lower level of absorption, the operating time of the two-stage “multicyclone-fiber baffle” system is much longer to reach the permissible resistance than for the same fiber material working in a single-stage system. This is due to the essence of the operation of the two-stage “inertia filter-baffle filter” filtration system. This explains the need for two-stage filters in vehicles operating under conditions of high dust concentrations in the air.
7. The originality of the developed test methodology lies in the fact that dust is applied to the filter material working behind the cyclone, and the granulometric composition of this dust is changed as a result of the actual air filtration process in the cyclone, characterized by the cyclone inlet speed, dust concentration, and suction rate. The methodology allows for the experimental determination of the characteristics of any fibrous filter materials predicted for the second stage of air filtration. These can be materials with any structural parameters, and the tests can be carried out over a wide range of changes in filtration conditions that correspond to the operation of an air filter under conditions of high dust concentration in the air.

Funding: This research received no external funding.

Data Availability Statement: Data is contained within the article.

Conflicts of Interest: The authors declare no conflict of interest.

References

1. Su, W.H. Dust and atmospheric aerosol. *Resour. Conserv. Recycl.* **1996**, *16*, 1–14. [CrossRef]
2. Bojdo, N.; Filippone, A. Effect of desert particulate composition on helicopter engine degradation rate. In Proceedings of the 40th European Rotorcraft Forum, Southampton, UK, 2–5 September 2014.
3. Smialek, J.L.; Archer, F.A.; Garlick, R.G. Turbine airfoil degradation in the persian gulf war. *JOM* **1994**, *46*, 39–41. [CrossRef]
4. Haig, C.; Hursthouse, A.; McIlwain, S.; Sykes, D. The effect of particle agglomeration and attrition on the separation efficiency of a Stairmand cyclone. *Powder Technol.* **2014**, *258*, 110–124. [CrossRef]
5. Dziubak, T.; Dziubak, S.D. A Study on the Effect of Inlet Air Pollution on the Engine Component Wear and Operation. *Energies* **2022**, *15*, 1182. [CrossRef]
6. Dziubak, T.; Karczewski, M. Experimental Studies of the Effect of Air Filter Pressure Drop on the Composition and Emission Changes of a Compression Ignition Internal Combustion Engine. *Energies* **2022**, *15*, 4815. [CrossRef]
7. Wróblewski, P. Reduction of friction energy in a piston combustion engine for hydrophobic and hydrophilic multilayer nanocoatings surrounded by soot. *Energy* **2023**, *271*, 126974. [CrossRef]
8. Wróblewski, P.; Rogólski, R. Experimental Analysis of the Influence of the Application of TiN, TiAlN, CrN and DLC1 Coatings on the Friction Losses in an Aviation Internal Combustion Engine Intended for the Propulsion of Ultralight Aircraft. *Materials* **2021**, *14*, 6839. [CrossRef] [PubMed]
9. Wróblewski, P.; Koszalka, G. An Experimental Study on Frictional Losses of Coated Piston Rings with Symmetric and Asymmetric Geometry. *SAE Int. J. Engines* **2021**, *14*, 853–866. [CrossRef]
10. Barris, M.A. *Total Filtration TM: The Influence of Filter Selection on Engine Wear, Emissions, and Performance*; SAE Technical Paper 952557; SAE: Warrendale, PA, USA, 1995.
11. Schaeffer, J.W.; Olson, L.M. Air Filtration Media for Transportation Applications. *Filtr. Sep.* **1998**, *35*, 124–129. [CrossRef]
12. Jaroszczyk, T.; Pardue, B.A.; Heckel, S.P.; Kallsen, K.J. Engine air cleaner filtration performance—Theoretical and experimental background of testing. In Proceedings of the AFS Fourteenth Annual Technical Conference and Exposition, Tampa, FL, USA, 1 May 2001. Included in the Conference Proceedings (Session 16).
13. Barbolini, M.; Di Pauli, F.; Traina, M. Simulation der luftfiltration zur auslegung von filterelementen. *MTZ* **2014**, *75*, 52–57. [CrossRef]
14. Dziubak, T. Zapylenie powietrza wokół pojazdu terenowego. *Wojsk. Przegląd Tech.* **1990**, *3*, 154–157. (In Polish)
15. Szczepankowski, A.; Szymczak, J.; Przynowa, R. The Effect of a Dusty Environment Upon Performance and Operating Parameters of Aircraft Gas Turbine Engines. In Proceedings of the Specialists' Meeting—Impact of Volcanic Ash Clouds on Military Operations NATO AVT-272-RSM-047, Vilnius, Lithuania, 17 May 2017.
16. Wasilewski, M.; Brar, L.S.; Ligus, G. Effect of the central rod dimensions on the performance of cyclone separators—Optimization study. *Sep. Purif. Technol.* **2021**, *274*, 119020. [CrossRef]
17. Nejad, J.V.N.; Kheradmand, S. The effect of arrangement in multi-cyclone filters on performance and the uniformity of fluid and particle flow distribution. *Powder Technol.* **2022**, *399*, 117191. [CrossRef]
18. Acharya, A.S.; Kurian, J.; Lowe, K.T.; Ng, W.F. Spectral Proper Orthogonal Decomposition Downstream of a Vortex Tube Separator. In Proceedings of the AIAA SciTech Forum, National Harbor, MD, USA, Online, 23–27 January 2023; Available online: <https://www.researchgate.net/publication/367311519> (accessed on 27 March 2023).
19. Fushimi, C.; Yato, K.; Sakai, M.; Kawano, T.; Kita, T. Recent Progress in Efficient Gas–Solid Cyclone Separators with a High Solids Loading for Large-scale Fluidized Beds. *KONA Powder Part. J.* **2021**, *38*, 94–109. [CrossRef]
20. Muschelknautz, U. Comparing Efficiency per Volume of Uniflow Cyclones and Standard Cyclones. *Chem. Ing. Tech.* **2020**, *93*, 91–107. [CrossRef]
21. Dziubak, T. Experimental Investigation of Possibilities to Improve Filtration Efficiency of Tangential Inlet Return Cyclones by Modification of Their Design. *Energies* **2022**, *15*, 3871. [CrossRef]
22. Dziubak, T.; Szwedkiewicz, S. Operating properties of non-woven fabric panel filters for internal combustion engine inlet air in single and two-stage filtration systems. *Eksploat. I Niezawodn. Maint. Reliab.* **2015**, *17*, 519–527. [CrossRef]
23. Dziubak, T. Experimental Studies of PowerCore Filters and Pleated Filter Baffles. *Materials* **2022**, *15*, 7292. [CrossRef] [PubMed]
24. Wei, S.; Qian, F.; Cheng, J.; Xiao, P.; Tang, L.; Jiang, R. Flow field analysis and structure optimization of honeycomb air filter. *Chin. J. Process Eng.* **2019**, *19*, 271–278. [CrossRef]
25. PowerCore®Air Intake Filters. Available online: <https://www.donaldson.com/en-us/engine/filters/products/air-intake/replacement-filters/powercore-filters/> (accessed on 27 March 2023).
26. Engine Air Cleaners, Service Parts and Accessories. Available online: <https://www.donaldson.com/content/dam/donaldson/engine-hydraulics-bulk/catalogs/air-intake/emea/f116005/Air-Intake-Product-Guide.pdf> (accessed on 27 March 2023).
27. Engine Air Filtration for Light, Medium, & Heavy Dust Conditions. Available online: <https://www.donaldson.com/content/dam/donaldson/engine-hydraulics-bulk/catalogs/air-intake/north-america/F110027-ENG/Air-Intake-Systems-Product-Guide.pdf> (accessed on 27 March 2023).
28. Yang, J.; Sun, G.; Gao, C. Effect of the inlet dimensions on the maximum-efficiency cyclone height. *Sep. Purif. Technol.* **2013**, *105*, 15–23. [CrossRef]
29. Duan, J.; Gao, S.; Lu, Y.; Wang, W.; Zhang, P.; Li, C. Study and optimization of flow field in a novel cyclone separator with inner cylinder. *Adv. Powder Technol.* **2020**, *31*, 4166–4179. [CrossRef]

30. Baltrėnas, P.; Chlebnikovas, A. Experimental research on the dynamics of airflow parameters in a six-channel cyclone-separator. *Powder Technol.* **2015**, *283*, 328–333. [[CrossRef](#)]
31. Jaroszczyk, T.; Ptak, T. Experimental Study of Aerosol Separation Using a Minicyclone. In Proceedings of the 10th Annual Powder and Bulk Solids Conference, O'Hare Expo Center, Rosemont, IL, USA, 7–9 May 1985.
32. Teng, G.; Shi, G.; Zhu, J. Influence of pleated geometry on the pressure drop of filters during dust loading process: Experimental and modelling study. *Sci. Rep.* **2022**, *12*, 20331. [[CrossRef](#)] [[PubMed](#)]
33. Allam, S.; Mimi Elsaid, A. Parametric Study on Vehicle Fuel Economy and Optimization Criteria of the Pleated Air Filter Designs to Improve the Performance of an I.C Diesel Engine: Experimental and CFD Approaches. *Sep. Purif. Technol.* **2020**, *241*, 116680. [[CrossRef](#)]
34. Saleh, A.M.; Tafreshi, H.V.; Pourdeyhimi, B. An analytical approach to predict pressure drop and collection efficiency of dust-load pleated filters. *Sep. Purif. Technol.* **2016**, *161*, 80–87. [[CrossRef](#)]
35. Saleh, A.M.; Vahedi Tafreshi, H. A simple semi-numerical model for designing pleated air filters under dust loading. *Sep. Purif. Technol.* **2014**, *137*, 94–108. [[CrossRef](#)]
36. Dziubak, T. Performance characteristics of air intake pleated panel filters for internal combustion engines in a two-stage configuration. *Aerosol Sci. Technol.* **2018**, *52*, 1293–1307. [[CrossRef](#)]
37. Seok, J.; Chun, K.M.; Song, S.; Lee, S. Study on the filtration behavior of a metal fiber filter as a function of filter pore size and fiber diameter. *J. Aerosol Sci.* **2015**, *81*, 47–61. [[CrossRef](#)]
38. Sun, Z.; Liang, Y.; He, W.; Jiang, F.; Song, Q.; Tang, M.; Wang, J. Filtration performance and loading capacity of nano-structured composite filter media for applications with high soot concentrations. *Sep. Purif. Technol.* **2019**, *221*, 175–182. [[CrossRef](#)]
39. Thomas, D.; Penicot, P.; Contala, P.; Leclerc, D.; Vendel, J. Clogging of fibrous filters by solid aerosol particles Experimental and modelling study. *Chem. Eng. Sci.* **2001**, *56*, 3549–3561. [[CrossRef](#)]
40. Walsh, D.C.; Stenhouse, J.I.T. The effect of particle size, charge, and composition on the loading characteristics of an electrically active fibrous filter material. *J. Aerosol Sci.* **1997**, *28*, 307–321. [[CrossRef](#)]
41. Bugli, N.J. *Service Life Expectations and Filtration Performance of Engine Air Cleaners*; No. 2000-01-3317; SAE Technical Paper; SAE: Warrendale, PA, USA, 2000.
42. Bugli, N. *Automotive Engine Air Cleaners—Performance Trends*; No. 2001-01-1356; SAE Technical Paper; SAE: Warrendale, PA, USA, 2001.
43. Durst, M.; Klein, G.; Moser, N. Filtration in fahrzeugen. In *Mannþhummel GMBH*; Mann þ Hummel GMBH: Ludwigsburg, Germany, 2005.
44. Taufkirch, G.; Mayr, G. Papierluftfilter für Motoren in Nutzfahrzeugen. *MTZ* **1984**, *45*, 95–105.
45. Melzer, H.H.; Brox, W. Ansauggerauschdampfer und Luftfilter für BMW 524 td. *MTZ* **1984**, *45*, 223–227.
46. Dziubak, T.; Bała, L.; Dziubak, S.D.; Sybilski, K.; Tomaszewski, M. Experimental Research of Fibrous Materials for Two-Stage Filtration of the Intake Air of Internal Combustion Engines. *Materials* **2021**, *14*, 7166. [[CrossRef](#)] [[PubMed](#)]
47. Needelman, W.; Madhavan, P. *Review of Lubricant Contamination and Diesel Engine Wear*; SAE Technical Paper; SAE: Warrendale, PA, USA, 1988. [[CrossRef](#)]

Disclaimer/Publisher's Note: The statements, opinions and data contained in all publications are solely those of the individual author(s) and contributor(s) and not of MDPI and/or the editor(s). MDPI and/or the editor(s) disclaim responsibility for any injury to people or property resulting from any ideas, methods, instructions or products referred to in the content.